Journal of Power Sources 247 (2014) 852–857

Contents lists available at ScienceDirect

Journal of Power Sources

journal homepage: www.elsevier.com/locate/jpowsour

Optimising heat treatment environment and atmosphere of electrolytic manganese dioxide for primary Li/MnO_2 batteries

Wesley M. Dose, Scott W. Donne*

Discipline of Chemistry, University of Newcastle, Callaghan, NSW 2308, Australia

HIGHLIGHTS

- Heat treated manganese dioxide is prepared under various heating environments and atmospheres.
- A mechanical tumbling environment, flowing air and O_2 atmospheres generated materials with high electrochemical performance.
- Materials with primary capacities up to 262 mAh g^{-1} and utilising 98% of Mn(IV) were obtained.

ARTICLE INFO

Article history:
Received 21 June 2013
Received in revised form
28 August 2013
Accepted 29 August 2013
Available online 14 September 2013

Keywords:
Lithium battery
Manganese dioxide
Heat treatment
Structural transformation

ABSTRACT

The influence of various conditions on the heat treatment step in preparing manganese dioxide for primary lithium batteries is reported. Heating environments considered are static air, flowing air and mechanical tumbling, while the heating atmospheres are flowing gases of air, O_2, N_2, Ar, 9:1 N_2/H_2, and under vacuum. The heat treated materials are characterised by the percentage of electrochemically active Mn(IV), cation vacancy and pyrolusite fractions, and BET surface area, which are the most influential parameters. Many materials made in this study show better electrochemical performance than literature materials, with primary capacities up to 263 mAh g^{-1} (2 mA g^{-1} discharge rate), which is 85% of the nominal MnO_2 utilisation, but 98% utilisation of the electrochemically active Mn(IV) species. In particular, changing the environment from static air to mechanical tumbling results in a significant increase in primary capacity, with the additional utilisation of 3–13% of the material across the 2–20 mA g^{-1} discharge rates, and up to 98% utilisation of Mn(IV). In addition, flowing air and oxygen atmospheres were also advantageous, with high primary capacities (260–262 mA g^{-1} at 2 mA g^{-1}) and excellent utilisation of the active material (up to 97% for flowing oxygen).

1. Introduction

Manganese dioxide (MnO_2) has been widely studied as a cathode material for lithium batteries since it is environmentally benign, cheap and abundant. These properties, coupled with its good electrochemical behaviour, have led to MnO_2 being the most widely used cathode material for commercial aqueous and non-aqueous battery systems [1]. Preparation of electrochemically active MnO_2 is commonly undertaken by electrolysis, and hence termed electrolytic manganese dioxide (EMD). Traditionally, EMD is described as having the γ-MnO_2 structure which is built up of edge- and corner-sharing MnO_6 octahedra to create an intergrowth of 1 × 1 (pyrolusite) and 2 × 1 (ramsdellite) tunnels extending in the c-direction through the structure [2,3]. Recent studies, however, employing transmission electron microscopy (TEM), electron diffraction and Rietveld refinement results of X-ray diffraction (XRD) have included ε-MnO_2 as either a component or the sole phase of EMD [4–6]. These differences may, at least partially, be explained by the fact that the difference between the above polymorphs is in the arrangement of the manganese within the octahedral sites of a hexagonal close packed oxygen array. Therefore, as highlighted by Simon et al. [7], EMD may be described as either: (i) a short range ordered γ-MnO_2 with microtwinning defects disrupting the short range order crystallites, or (ii) a long range disordered ε-MnO_2 as a result of manganese disorder throughout the long range oxygen framework.

Irrespective of the structural model best describing EMD, this material must be heat treated prior to use in lithium batteries. The effect this has on the structure has been well documented from the traditional perspective, that is, upon heating EMD (γ-MnO_2) is

* Corresponding author. Tel.: +61 2 4921 5477; fax: +61 2 4921 5472.
E-mail address: scott.donne@newcastle.edu.au (S.W. Donne).

0378-7753/$ – see front matter © 2013 Elsevier B.V. All rights reserved.
http://dx.doi.org/10.1016/j.jpowsour.2013.08.142

converted towards β-MnO_2 to what has been described as a γ/β-MnO_2 phase [8–10]. In addition, heat treatment also results in the removal of the problematic water content, present as surface water and protons associated with vacancy and Mn(III) structural defects [11–13]. Lee et al. [14,15] identified three types of water in EMD using temperature programmed desorption (TPD): Type 1 water, which is physisorbed water able to be reversibly removed around 100 °C; Type 2 water, which is comprised of surface bound hydroxyls and water of crystallisation that is irreversibly removed around 200 °C; and Type 3 water, which are bulk hydroxyl groups removed irreversibly at 300 °C. The effect of three heating atmospheres (oxygen, nitrogen and helium) on the water loss revealed an oxygen atmosphere was most useful for observing the removal of Type 3 water, since the partial pressure of oxygen delays the main lattice decomposition. Chemisorption of oxygen in this atmosphere also resulted in a perceived lower amount of loss of Type 2 water.

Heat treatment atmosphere and environment are significant factors in determining the properties of the heated product. For the decomposition reactions of MnO_2 (Eq. (1)), this has been studied extensively (e.g., [16–18] and reviewed in Ref. [19]).

$$MnO_2 \xrightarrow{450\ ^\circ C} Mn_2O_3 \xrightarrow{950\ ^\circ C} Mn_3O_4 \xrightarrow{1300\ ^\circ C} MnO \quad (1)$$

Heat treatment of MnO_2 for use in lithium batteries, however, is most often conducted between 250 °C and 400 °C, a temperature window in which the influence of heating atmosphere and environment on the MnO_2 properties has not, to our knowledge, been studied in detail. Therefore, the objective of this work is to investigate the effect of the heating conditions on the heat treated EMD (HEMD) properties and the subsequent electrochemical performance of these materials in primary Li/MnO_2 cells. Understanding these relationships represents an important step in optimising the performance of HEMD in lithium batteries. The influence of the heating environment will be investigated in this work by comparing MnO_2 prepared with a static air environment, flowing air environment and mechanical tumbling of material particles. Heating atmospheres considered will be flowing gases of air, O_2, N_2, Ar, 9:1 N_2/H_2, and under an applied vacuum.

2. Experimental

The EMD used in this work was prepared by the anodic electrolysis (65 A m^{-2}) of an acidic (0.25 M H_2SO_4) solution of $MnSO_4$ (1.0 M) at 97 °C. After deposition the solid EMD was mechanically removed from the substrate (titanium), washed thoroughly to neutralise any entrained electrolyte and then milled to a −105 μm powder. The details of this process have been described previously [20].

The method of kinetic analysis, based on TG experiments, to determine the necessary isothermal heating time to remove the problematic water content from the EMD structure has been outlined in detail in our earlier work [20]. The heat treatment regimes were carried out by heating ~10 g of EMD in a MTI GSL1300X tube furnace. The temperatures and times for the heat treatment are listed in Table 1. Flowing environments were created by passing the required gas over the sample at ~100 mL min^{-1}. The vacuum environment was achieved by placing the EMD in a sealed cylindrical cell which was evacuated with a vacuum pump throughout the experiment. The influence of a rotating environment was tested by placing EMD in the same sealed cylindrical cell which was turned continually within the tube furnace throughout the heating experiment at a sufficient rate to ensure the tumbling of particles.

The properties of each material generated were characterised by X-ray diffraction to determine structure, gas adsorption to determine BET surface area and morphology, and potentiometric titration to determine chemical composition (see Ref. [21] for methods). Electrochemical properties of the samples were measured using CR2032 coin-type cells assembled in a dry argon filled glove box. The working electrode was fabricated by compressing a 1:8:1 mixture (by weight) of EMD, graphite and binder (polyvinylidene fluoride), respectively, into a pellet 1 cm in diameter and ~1 mm thickness, which was subsequently dried at 110 °C under vacuum for 12 h and then transferred to the glove box. Lithium foil served as the anode, while a Celgard 2400 sheet was employed as a separator. The electrolyte was a solution of 1 M $LiPF_6$ in 1:1 w/w ethylene carbonate/dimethyl carbonate. Using galvanostatic mode, the cells were tested by a Perkin Elmer VMP2 multichannel potentiostat at room temperature. Discharge rates considered were 2, 5, 10 and 20 mA g^{-1} of MnO_2. Discharge capacities are quoted in two ways; the fraction of the theoretical utilisation of MnO_2 utilised, and the fraction of the active material, Mn(IV), utilised. The fraction of Mn(IV) used here was calculated from the potentiometric titration method used to determine chemical composition [21].

Table 1
Optimum heat treatment temperatures and times for the EMD used in this work, as determined by kinetic analysis.

Temperature (°C)	Time (h)
200	31.65
250	11.12
300	5.07
350	1.52
400	0.27

3. Results and discussion

Numerous material properties can be obtained from the experimental techniques employed in the characterisation of HEMD samples prepared in this work. While all these properties cannot be considered in detail here, in previous work [22] it was found that the most significant material properties determining the electrochemical capacity were the percentage of active material (Mn(IV)), cation vacancy fraction, pyrolusite fraction and BET surface area. Therefore, this selection of properties is used to compare and contrast the composition, structure and morphology of the HEMD samples prepared under different environments and atmospheres.

3.1. Heating environment

The properties of the HEMD materials heated in a static, flowing and tumbling environment are shown in Fig. 1. The non-linear change in these properties with respect to temperature is a consequence of the different heating time used at each temperature (Table 1). These heating times were calculated using kinetic analysis based on the mass loss due to structural water removal from the starting EMD [20]. As a consequence, the material properties measured are a function of heating temperature and heating time. An example of this can be observed in the Mn(III) percentage data, which is determined by the complex interplay between the kinetics of Mn(III) oxidation at different temperatures (the effects of temperature and time) and the thermal reduction of MnO_2 to Mn_2O_3 at high temperature.

Fig. 1 clearly demonstrates that changing from a static environment to a flowing one generally results in a lower Mn(III) percentage, higher cation vacancy fraction and less structural transformation (manifested in a lower pyrolusite fraction). This

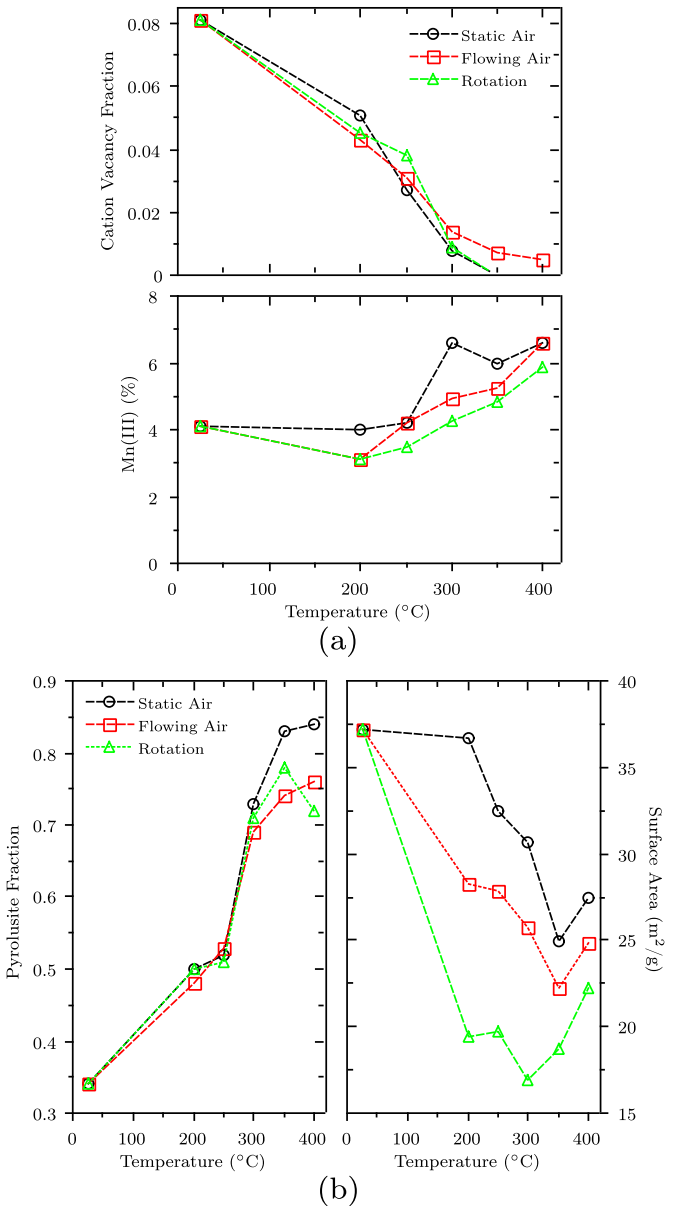

Fig. 1. Properties of the HEMD materials heat treated under a static air, flowing air and tumbling environment. Shown are the percentage Mn(III), cation vacancy fraction, pyrolusite fraction and surface area.

behaviour is likely the combined influence of two effects. Firstly, a flowing environment is better able to remove the gases that are produced in the removal of water from the structure and the associated exothermic structural transformation [18,19]. These gases are the heat carriers for the system and therefore their removal transports the heat produced away from the sample. The main gas product would be H_2O, which even in the gaseous phase has a relatively high heat capacity (34 J K^{-1} mol^{-1} [23]), making heat removal quite effective. The removal of this excess heat likely contributes to the lower percentage Mn(III) observed, since less thermal decomposition of the MnO_2 to lower oxidation states, such as Mn_2O_3, will occur under these conditions. A lower pyrolusite fraction also results from the removal of excess heat since the reaction to more pyrolusitic materials is thermally driven.

The second factor influencing this behaviour is the relative potential of the atmospheres created in static versus flowing air environments. The flowing environment replenishes the oxidising component of the air and therefore a higher potential for the atmosphere/sample system is maintained throughout the experiment. This favours higher potential structures (γ-MnO_2 over γ/β-MnO_2) and high potential defects (cation vacancies over their annealment, and Mn(IV) over Mn(III)). Since the structural conversion, annealing of vacancies and reduction of Mn(IV) are all thermally driven, however, these processes still occur in the flowing environment, albeit to a lesser extent.

Comparing mechanical tumbling during heating to the static environment reveals tumbling has resulted in significantly lower amounts of Mn(III) and lower pyrolusite fractions, especially at the higher temperatures. This is the result of the additional exposure of individual particles to the atmosphere which aids in the removal of excess heat generated in the structural conversion and water loss processes.

The surface area of HEMD is also affected by the heating environment. A flowing environment decreases the surface area from that of a static one, while mechanical tumbling decreases this even further. These environments clearly promote the removal of pores in the process of Mn(IV) diffusion through the structure as a more defect free and crystalline structure is formed. The reason for the increased rate of inter-diffusion between crystallites in flowing and mechanical tumbling environments is, at this stage, not known.

In summary, the slightly greater retention of the γ-MnO_2 structure coupled with lower proportions of Mn(III) for HEMD prepared in the flowing and rotating environment are both likely more favourable material properties for high electrochemical performance, as will be discussed in Section 3.3.

3.2. Heating atmosphere

The effect of heating atmosphere on the properties of the HEMD materials is shown in Fig. 2. It should be noted that materials generated under the flowing N_2/H_2 atmosphere have not been characterised beyond collecting XRD patterns of the heated products. This atmosphere was included to ensure that the influence of oxidising, inert and reducing atmospheres on the heat treated products were all considered. Even the mild reducing atmosphere used in this work (9:1 mixture of nitrogen to hydrogen) was found to drastically lower the decomposition temperature of the MnO_2. Even heat treatment at 250 °C resulted in the reduction of the material from MnO_2 to Mn_3O_4 (see Fig. 3), a transition which does not take place below 950 °C in air [18]. Further, heat treatment at 350 °C for 1.52 h resulted in a material with both Mn_3O_4 and MnO phases evident in the XRD pattern (Fig. 3). Longer heating times may allow for the full conversion of the material to MnO at 350 °C. Notably, in both these instances the decomposition temperature has been significantly lowered, by at least 700 °C for the 250 °C heat treatment and by as much as 950 °C for the 350 °C treatment.

The lowering of the decomposition temperature for MnO_2 in different atmospheres has been noted previously in the literature. For instance, the use of a N_2 atmosphere rather than air results in the decomposition temperature decreasing from 546 °C to 473 °C [18]. This effect can be understood from consideration of the equilibrium between MnO_2 and Mn_2O_3: $MnO_2 \rightleftharpoons Mn_2O_3 + 1/2O_2$. In an oxygen containing atmosphere, the equilibrium will be shifted to the left hand side, prolonging the presence of MnO_2. On the contrary, with an inert nitrogen atmosphere, the equilibrium is shifted to the right-hand side at a lower relative temperature. Further, DSC measurements taken under a reducing 1:3 hydrogen–nitrogen purge gas brings the MnO_2 decomposition temperature lowered to 300 °C, and complete reduction to MnO by 450 °C [17].

The materials produced under the remaining atmospheres all yielded compounds with stoichiometry close to MnO_2 ($x > 0.91$ for

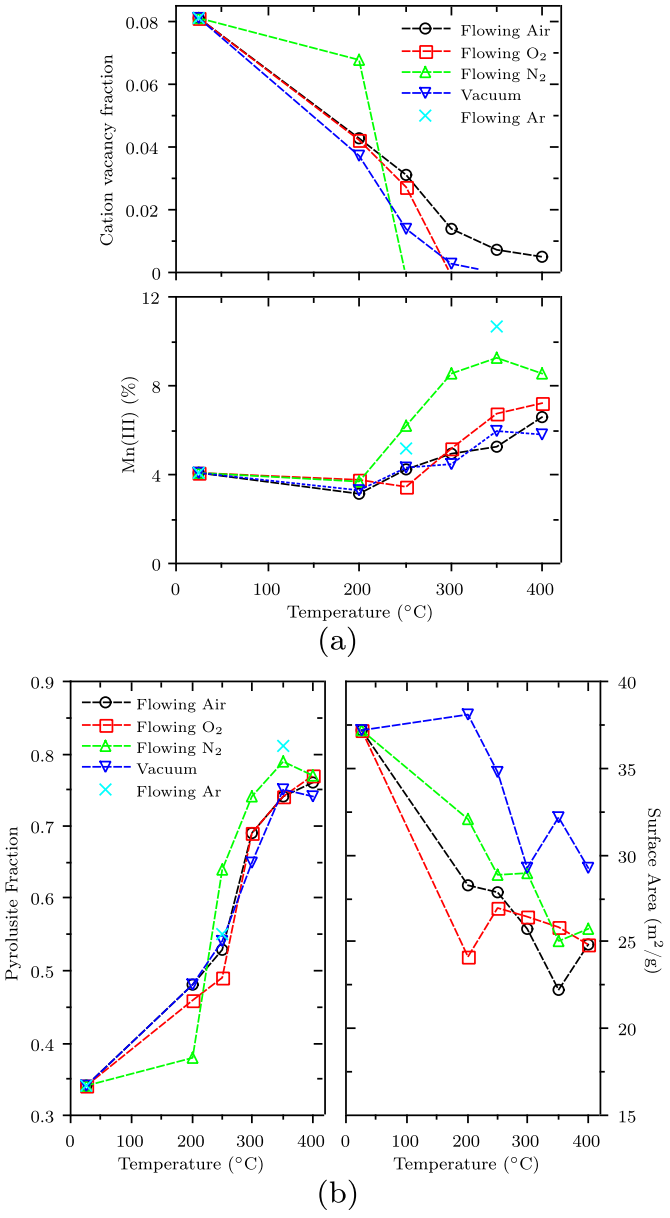

Fig. 2. Properties of the HEMD materials heat treated under atmospheres of flowing air, oxygen, nitrogen, argon and an applied vacuum. Shown are the percentage Mn(III), cation vacancy fraction, pyrolusite fraction and surface area.

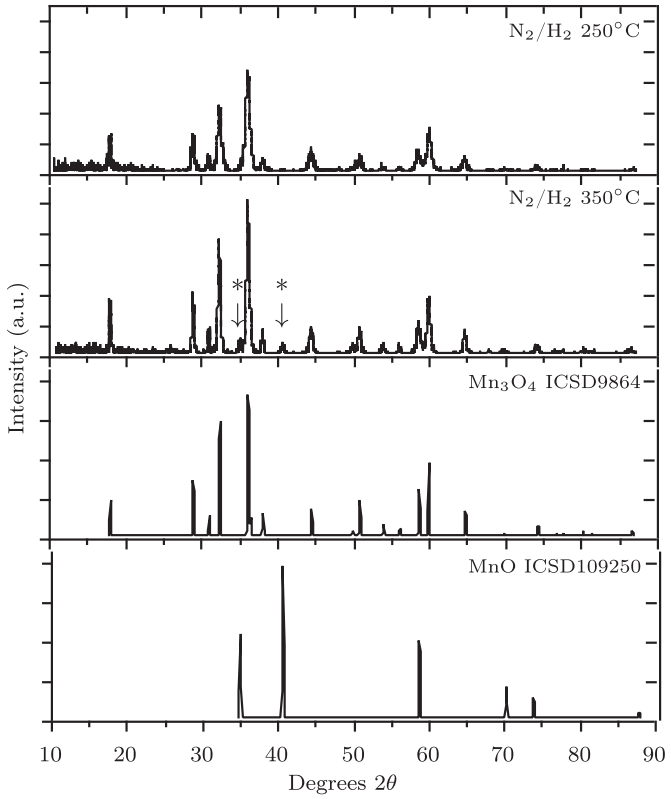

Fig. 3. X-ray diffraction patterns for the samples prepared under flowing N_2/H_2 (9:1) at 250 and 350 °C, and ICSD reference patterns showing the Mn_3O_4 and MnO structures. The symbol (*) highlights MnO peaks distinguishable in the N_2/H_2 350 °C material.

x in MnO_x). Fig. 2 show that there is little difference in composition and structure in materials prepared under air and oxygen. The applied vacuum gave similar values for Mn(III) and pyrolusite fraction, although resulted in a lower vacancy fraction as the removal of the associated structural water (present as protons) is enhanced in the vacuum conditions. This allows greater proton diffusion and extraction to take place during the heating period.

As shown in Fig. 2, atmospheres of flowing nitrogen and argon generally result in higher Mn(III) percentage and pyrolusite content, while cation vacancies are completely removed at lower temperatures, compared to the other atmospheres. The relative potential created by the sample and the surrounds under the nitrogen and argon atmospheres, compared to oxygen and air, likely explains these differences. Nitrogen and argon are inert gases and therefore do not contribute to the potential of the sample/atmosphere system. Thus the potential of the system is determined solely by the sample. Conversely, in oxygen and air the atmosphere influences the potential of the sample/atmosphere system, increasing this value as a result of the oxidising component present. As a result, higher potential structures and defects are promoted in oxygen and air, while nitrogen and argon favour the lower potential forms, namely, pyrolusite over ramsdellite, Mn(III) over Mn(IV) and lower fractions of vacancy defects.

The removal of cation vacancies at lower heating temperatures are of particular interest since although the inclusion of these defects has been reported to give a higher potential battery material [12], the structural water associated with the vacancy is detrimental to electrochemical performance in non-aqueous batteries [8] and they lower the charge density. In light of the higher percentage of electrochemically inactive Mn(III) also promoted under these conditions, however, one does not necessarily anticipate their superior performance (in terms of mAh g^{-1} of MnO_2) in Li/MnO_2 batteries.

The gaseous atmosphere used during the heating regime has also impacted upon the heat treated material surface area (Fig. 2). Materials heat treated under atmospheres of flowing air and oxygen show similar trends in BET surface area, with values lying in the range 24–28 $m^2\ g^{-1}$. The inert atmosphere generated by flowing nitrogen has generally led to higher BET surface area, with an average increase of ~2.5 $m^2\ g^{-1}$ over the air and oxygen atmospheres, and further increases were observed when a vacuum is applied during heat treatment (average increase of ~8 $m^2\ g^{-1}$).

3.3. Electrochemical performance

HEMD prepared at 350 °C under the different environments and atmospheres is used as an example to link the material properties to electrochemical performance. This heat treatment temperature

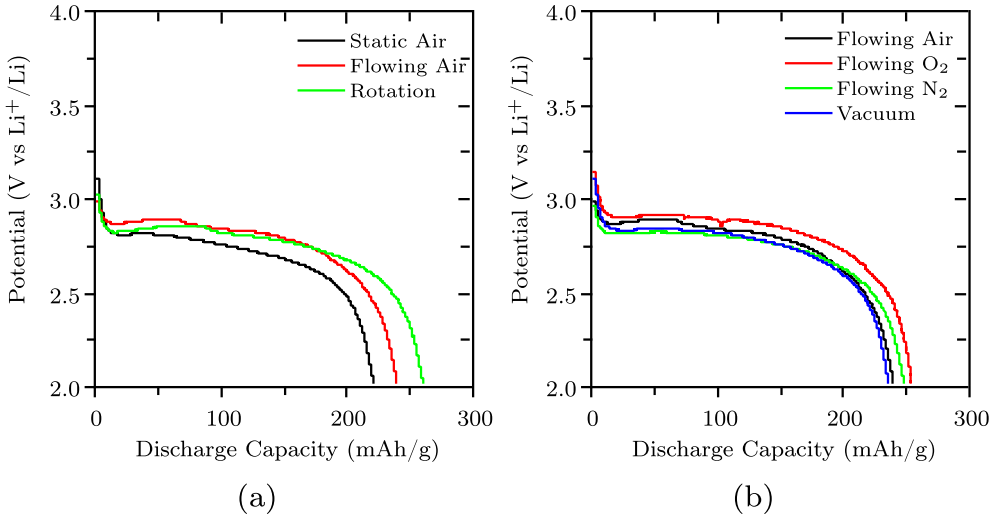

Fig. 4. Representative discharge curves for manganese dioxides heated at 350 °C under various (a) environments and (b) atmospheres, discharged at a 5 mA g^{-1} rate.

was selected since it led to some of the highest performing HEMDs. A selection of representative discharge curves for heating environment and atmosphere for the 350 °C material discharged at 5 mA g^{-1} are shown in Fig. 4. The primary capacity of the materials at four discharge rates, 2, 5 10 and 20 mA g^{-1}, is represented in Fig. 5 in two ways: (i) as the fraction of the theoretical utilisation of MnO_2, being 308 mAh g^{-1} (strong data), and (ii) the fraction of the active material, Mn(IV), utilised (faded data).

3.3.1. Heating environment

The primary capacity of the materials prepared under static, flowing and mechanical tumbling environments are shown in Fig. 5a. This clearly shows that flowing and mechanical tumbling environments promote favourable HEMD material characteristics to improve electrochemical performance. For MnO_2 utilisation at the 2 mA g^{-1} rate this represents an additional 3% utilisation, or an increase from 253 mAh g^{-1} to 262 mAh g^{-1}. The improvement over a static environment (169 mAh g^{-1}) is more pronounced at higher discharge rates, with an additional 6% for a flowing environment (188 mAh g^{-1}), and 13% for a tumbling environment (209 mAh g^{-1}), at 20 mA g^{-1}.

Consideration of the utilisation of the active Mn(IV) present gives insight as to the extent of the optimisation achieved using a mechanical tumbling environment over either a static or flowing environment. At 2 mA g^{-1} 98% of the Mn(IV) is reduced in the primary discharge, while 78% is utilised when the discharge rate is increased to 20 mA g^{-1}. This is an extra 14% of the active material which has been utilised compared to using a static environment.

As discussed above, HEMD prepared under flowing and rotating environments has a lower Mn(III) content and higher retention of the γ-MnO_2 structure. Mn(III) is electrochemically limiting and has with it an associated proton which is detrimental to performance. While differing amounts of Mn(III) can partially explain the differences between the utilisation of the MnO_2 present (black data), it does not account for the variation in the fraction of Mn(IV) utilised (grey data). A higher fraction of the γ-phase may account for this difference. The γ-phase, which is an intergrowth of ramsdellite (2 × 1 tunnels) and pyrolusite (12 × 1 tunnels), is likely less

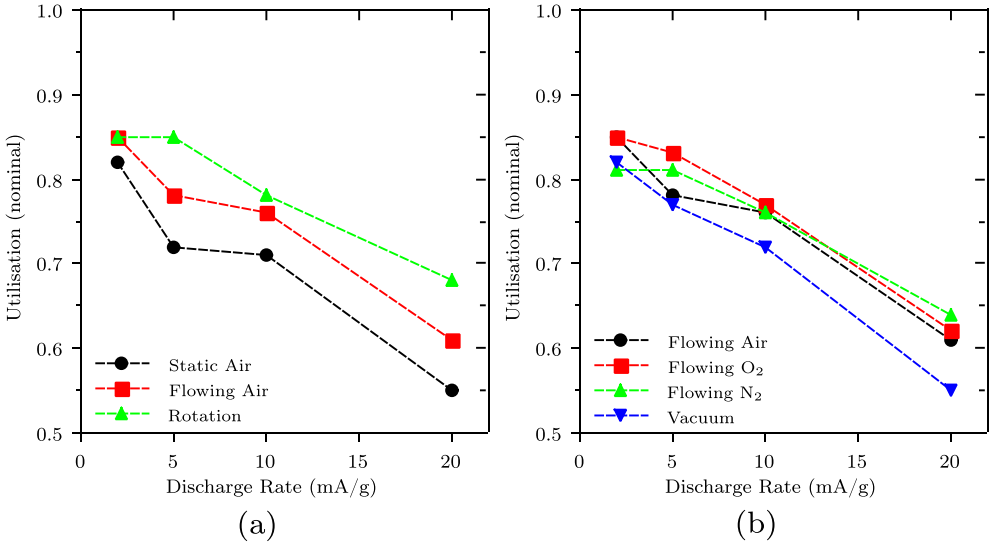

Fig. 5. Electrochemical capacity of manganese dioxides heated at 350 °C under various (a) environments and (b) atmospheres discharged at 2, 5 10 and 20 mA g^{-1}. The theoretical utilisation of MnO_2 (strong data) and the fraction of electrochemically active Mn(IV) utilised (faded data) are shown.

inhibiting to Li diffusion through the material and thereby facilitates the more complete utilisation of the core of crystallites. This would especially aid the performance at higher discharge rates, as is clearly the case for the HEMD prepared with mechanical tumbling.

3.3.2. Heating atmosphere

Fig. 5b shows the primary capacity for the HEMDs heated under different atmospheres. Heating under flowing air or flowing oxygen generally gave the highest performing materials across the discharge rates considered. HEMD prepared under flowing nitrogen resulted in poorer performance at 2 mA g^{-1}, but had capacities similar or higher than air or oxygen at higher discharge rates. Materials heated under vacuum gave poorest performance at all rates, with 3–6% less utilisation of MnO_2. The performance of the vacuum prepared HEMD was in fact very similar to the HEMD made under static air conditions, with each being the poorest environment or atmosphere tested.

Utilisation of the active material gives a particular advantage to the flowing nitrogen HEMDs, which as discussed above, have a high percentage of Mn(III). This demonstrates that 97% of the Mn(IV) present is reduced at the 2 mA g^{-1} discharge rate, and at higher rates these materials give the highest utilisation of active material compared to the other atmospheres.

The influence of individual HEMD properties on the primary capacity of the material has previously been examined [24]. In this study it was found that, as was to be expected, a lower percentage of Mn(III) was favourable, given that less Mn(III) implies more Mn(IV), which is the electrochemically active oxidation state. The data also suggested, however, that higher amounts of Mn(III) (>8%) could also contribute in a positive way to the primary capacity. While the reason for this at this stage remains unclear, the data collected here for the HEMD prepared under flowing nitrogen may be further confirmation of this effect.

The flowing oxygen materials utilise a high percentage of the available Mn(IV) and utilise the highest fraction of MnO_2 present at most discharge rates, therefore offering overall better performance characteristics than the flowing nitrogen HEMDs. Flowing air materials also have excellent capacities, although not utilising as high a fraction of the Mn(IV) present compared to the flowing oxygen materials. It is difficult to attribute the performance of the flowing oxygen and air HEMDs to any one characteristic. In all probability, it is a combination of near-ideal properties which give these materials the improved performance observed.

4. Conclusions

In this work, the effect of the heat treatment environment and atmosphere on the physical properties and electrochemical performance of heat treated manganese dioxide is investigated. Changing the heating environment from static air to flowing air results in a HEMD with less Mn(III), more cation vacancies and a lower fraction of pyrolusite, while a mechanically tumbling environment has the effect of significantly lowering the Mn(III) percentage and pyrolusite fraction. The heating atmosphere also impacts on the properties of the HEMD, with excellent removal of cation vacancies under flowing nitrogen and vacuum conditions, and higher Mn(III) and lower cation vacancy fractions in inert (Ar and N_2) atmospheres. HEMDs prepared under oxidising atmospheres of flowing air and flowing oxygen yield very similar material properties, while a slightly reducing atmosphere (9:1 N_2/H_2) dramatically reduced the decomposition temperature making the products undesirable for application in Li/MnO_2 batteries.

The electrochemical results presented in this paper highlight the importance of selecting the ideal heating environment and atmosphere. Superior performance came from HEMD materials prepared with mechanical tumbling, with additional utilisation over a static air environment of 3–13% within the 2–20 mA g^{-1} discharge rate range. Further, utilisation of the active Mn(IV) is very high for these materials, 98% at 2 mA g^{-1}. A distinct advantage is also found for materials heated under atmospheres of flowing air and flowing oxygen, which give high capacities (262 mAh g^{-1} at 2 mA g^{-1}) and high utilisation of the active Mn(IV) present (97% for flowing oxygen at 2 mA g^{-1}).

Acknowledgements

WMD acknowledges the UoN for the provision of an APA PhD scholarship. Thanks are also extended to the UoN EM-X-ray unit for assistance in obtaining the XRD data.

References

[1] D. Linden, T.B. Reddy, Handbook of Batteries, third ed., McGraw Hill, New York, 2002.
[2] P.M. de Wolff, Acta Crystallogr. 12 (1959) 341–345.
[3] Y. Chabre, J. Pannetier, Prog. Solid State Chem. 23 (1995) 1–130.
[4] A.H. Heuer, A.Q. He, P.J. Hughes, F.H. Feddrix, ITE Lett. Batt. New Tech. Med. 1 (2000) 926–930.
[5] C.-H. Kim, Z. Akase, L. Zhang, A.H. Heuer, A.E. Newman, P.J. Hughes, J. Solid State Chem. 179 (2006) 753–774.
[6] D.E. Simon, T.N. Andersen, C.D. Elliott, ITE Lett. Batt. New Tech. Med. 1 (2000) 372–381.
[7] D.E. Simon, R.W. Morton, J.J. Gislason, Adv. X-ray Anal. 47 (2004) 267–280.
[8] H. Ikeda, T. Saito, H. Tamura, in: Manganese Dioxide Symp. [Proc.], vol. 1, 1975, pp. 384–401.
[9] Y. Shao-Horn, S.A. Hackney, B.C. Cornilsen, J. Electrochem. Soc. 144 (1997) 3147–3153.
[10] W. Bowden, C. Grey, S. Hackney, X.Q. Yang, Y. Paik, F. Wang, T. Richards, R. Sirotina, ITE Lett. Batt. New Tech. Med. 3 (2002) 312–336.
[11] P. Ruetschi, J. Electrochem. Soc. 131 (1984) 2737–2744.
[12] P. Ruetschi, J. Electrochem. Soc. 135 (1988) 2657–2663.
[13] P. Ruetschi, R. Giovanoli, J. Electrochem. Soc. 135 (1988) 2663–2669.
[14] J.A. Lee, C.E. Newnham, F.L. Tye, J. Colloid Interface Sci. 42 (1973) 372–380.
[15] J.A. Lee, C.E. Newnham, F.S. Stone, F.L. Tye, J. Colloid Interface Sci. 45 (1973) 289–294.
[16] F. Tedjar, J. Guitton, Thermochim. Acta 181 (1991) 13–22.
[17] C. Gonzalez, J.I. Gutierrez, J.R. Gonzalez-Velasco, A. Cid, A. Arranz, J.F. Arranz, J. Therm. Anal. Calorim. 52 (1998) 985–989.
[18] B. Liu, P.S. Thomas, A.S. Ray, R.P. Williams, J. Therm. Anal. Calorim. 76 (2004) 115–122.
[19] B.D. Desai, J.B. Fernandes, V.N.K. Dalal, J. Power Sources 16 (1985) 1–43.
[20] W.M. Dose, S.W. Donne, J. Therm. Anal. Calorim. 105 (2011) 113–122.
[21] W.M. Dose, S.W. Donne, Mat. Sci. Eng. B 176 (2011) 1169–1177.
[22] W.M. Dose, S.W. Donne, J. Power Sources 221 (2013) 261–265.
[23] G. Aylward, T. Findlay (Eds.), SI Chemical Data, fifth ed., John Wiley & Sons Australia, Australia, 2002.
[24] W.M. Dose, S.W. Donne, Electrochim. Acta 105 (2013) 305–313.